

DOI: 10.19884/j.1672-5220.202207005

Synthesis and Characterization of Polyborosilazane for Silicoboron-Carbonitride Ceramic

MALIK Hamza¹, SHEN Jian¹, TANG Zicheng¹, LIU Yong^{1,2*}

1. State Key Laboratory for Modification of Chemical Fibers and Polymer Materials, College of Materials Science and Engineering, Donghua University, Shanghai 201620, China

2. Key Laboratory of High-Performance Fiber and Product, Ministry of Education, Donghua University, Shanghai 201620, China

Abstract: A silicoboron-carbonitride (SiBNC) ceramic precursor, polyborosilazane (PBSZ), was successfully synthesized using boron trichloride (BCl_3), trichlorosilane (HSiCl_3) and hexamethyldisilazane ($\text{Me}_6\text{Si}_2\text{NH}$) as raw materials through the polymer-derived ceramics (PDCs) method. Fourier transform infrared (FTIR) spectroscopy, nuclear magnetic resonance (NMR), X-ray photoelectron spectroscopy (XPS), thermogravimetric analysis (TGA) and differential scanning calorimeter (DSC) were used to analyze the structure and high-temperature performance of the obtained PBSZ. Results showed that the network of silicon nitrogen boron (Si—N—B) and six-membered boron nitrogen (B—N) rings were presented in the PBSZ structure. The ceramic yield of the synthesized PBSZ at 800 °C in a nitrogen atmosphere was 53.9%.

Key words: silicoboron-carbonitride (SiBNC) ceramic; ceramic precursor; polyborosilazane (PBSZ); polymer-derived ceramics (PDCs) method

CLC number: TQ174.1

Document code: A

Article ID: 1672-5220(2024)03-0257-06

Open Science Identity
(OSID)

0 Introduction

Silicoboron-carbonitride (SiBNC) ceramics are extremely promising materials for applications in extreme environments due to their excellent thermal properties, high mechanical properties, and excellent oxidation and creep resistance characteristics^[1-4]. Several studies proved that the SiBNC quaternary system exhibited excellent high-temperature performance as compared to binary and ternary ceramics^[5-7]. The research showed that the decomposition temperature was about 2 000 °C for the SiBNC ceramics with 5.9% (mass fraction) boron, while for SiCN ceramics it was only about 1 500 °C^[8]. The presence of boron in SiBNC ceramics confers the ceramics with low density and superior thermal properties, making them

ideally suited for aerospace and aviation applications^[8-9]. Nevertheless, the very low diffusion coefficients of silicon (Si) and boron (B) necessitate the use of the polymer-derived ceramics (PDCs) method as an effective approach for synthesizing SiBNC ceramics^[8,10-12]. Consequently, the preparation of high-performance polyborosilazane (PBSZ) is crucial for achieving the high-temperature performance of SiBNC ceramics^[11,13-14].

To improve the performance of PBSZ, researchers have synthesized different kinds of PBSZ. Zhao et al.^[8] synthesized high-yield PBSZ by using different polymer routes. Soluble and meltable hyperbranched PBSZ with Si—H and $\text{CH}=\text{CH}_2$ was synthesized by Kong et al.^[15]. $\text{B}(\text{C}_2\text{H}_4\text{SiCH}_3\text{NCH}_3)_3$ was prepared by Bernard et al.^[16] via aminolysis of $\text{B}(\text{C}_2\text{H}_4\text{SiCH}_3\text{Cl}_2)_3$. Borazine precursors were synthesized by Jäschke et al.^[17] via cross-linking of $\text{Cl}_3\text{SiCH}_2\text{BCl}_2$, $(\text{CH}_3)_2\text{Cl}_2\text{SiCH}_2\text{BCl}_2$ and methylamine. The obtained SiBNC ceramics exhibit excellent thermal properties and oxidation resistance at temperatures up to 1 300 °C. However, it is difficult to avoid moisture and keep the complete process in an inert atmosphere during multiple-step processes.

Herein, a PBSZ for SiBNC ceramic is synthesized by using boron trichloride (BCl_3), trichlorosilane (HSiCl_3) and hexamethyldisilazane ($\text{Me}_6\text{Si}_2\text{NH}$) as raw materials through the polymer-derived ceramics (PDCs) method. In addition, the structure and properties of the synthesized PBSZ are analyzed.

1 Materials and Methods

1.1 Materials

Nitrogen gas with 99.99% purity in volume was supplied by Shanghai Shenzhong Industrial Gas Co., Ltd., China. BCl_3 with 99.5% purity in volume was supplied by Beijing Multi-Technology Co., Ltd., China. HSiCl_3 with 99.7% purity and $\text{Me}_6\text{Si}_2\text{NH}$ with 99%

Received date: 2022-07-24

Foundation item: Key Laboratory of National Defense Science and Technology, China (No. 6142906190510)

* Correspondence should be addressed to LIU Yong, email: liuyong@dhu.edu.cn

Citation: MALIK H, SHEN J, TANG Z C, et al. Synthesis and characterization of polyborosilazane for silicoboron-carbonitride ceramic[J]. *Journal of Donghua University (English Edition)*, 2024, 41(3): 257-262.

purity in volume were supplied by Bailingwei Chemical Technology Co., Ltd., China.

1.2 Synthesis of PBSZ

PBSZ were synthesized from BCl_3 , HSiCl_3 and $\text{Me}_6\text{Si}_2\text{NH}$, and the mass ratio of HSiCl_3 to BCl_3 to $\text{Me}_6\text{Si}_2\text{NH}$ is 3 : 2 : 15. Due to the violent and highly exothermic nature of the reaction, the raw materials were carefully added to the flask simultaneously and slowly at $-30\text{ }^\circ\text{C}$. The evaporation of byproducts and n-hexane took place at $80\text{ }^\circ\text{C}$ for 2 h. To obtain PBSZ with appropriate viscosity, the flask was subsequently heated at a rate of $20\text{ }^\circ\text{C}/\text{h}$ up to $200\text{--}250\text{ }^\circ\text{C}$, then maintained at $200\text{--}250\text{ }^\circ\text{C}$ for 2 h.

1.3 Characterization

The Fourier transform infrared (FTIR) spectrometer (Nicolet 6700, USA), the KBr pellet method and the attenuated total reflection (ATR) method were used to analyze the structure of PBSZ. The scanning wavenumber range is $4\,000\text{--}500\text{ cm}^{-1}$, and the number of scans is 32. The nuclear magnetic resonance (NMR) spectra (^1H , ^{11}B , ^{13}C and ^{29}Si) of PBSZ were analyzed by an NMR spectrometer (Avance 400/600, Switzerland). The frequencies of the ^1H , ^{11}B , ^{13}C and ^{29}Si spectra are 100.60, 79.50, 128.37 and 400.13 MHz, respectively. The X-ray photoelectron spectroscopy (XPS) measurements were conducted on an XPS instrument (Escalab250, USA). The degree of vacuum is $2\times 10^{-7}\text{ Pa}$ and the sample surface was sputtered for 10 min at an energy of 0.9 eV and a signal-to-noise ratio of 30 : 1. The thermogravimetric analysis (TGA) of PBSZ was analyzed on a TGA instrument (TG209 F1, Germany). PBSZ was heated to $800\text{ }^\circ\text{C}$ at a constant temperature of $10\text{ }^\circ\text{C}/\text{min}$ in a nitrogen atmosphere, and the gas flow rate was $20\text{ mL}/\text{min}$. The density of PBSZ was measured by an automatic true density analyzer (1000UPY-20 T, American), under the conditions of N_2 protection, and the gas flow rate was $50\text{ mL}/\text{min}$, the heating rate was $10\text{ }^\circ\text{C}/\text{min}$, the temperature range was $50\text{--}250\text{ }^\circ\text{C}$, and the sample amount was 5–10 mg. The glass transition temperature and melting point of PBSZ were tested by differential scanning calorimeter (DSC) (TADSC250, USA).

2 Results and Discussion

2.1 FTIR analysis of PBSZ

FTIR spectroscopy is used to analyze the structure of

PBSZ. As shown in Fig. 1, the peaks at about $3\,440\text{ cm}^{-1}$ and $1\,230\text{ cm}^{-1}$ are caused by the N—H vibration. The peak observed at $2\,190\text{ cm}^{-1}$ is assigned to the Si—H bond, and the signal observed at $1\,430\text{ cm}^{-1}$ is attributed to the Si—C bond. While the stretching vibration peaks at $2\,930\text{ cm}^{-1}$ and 780 cm^{-1} are assigned to the C—H bond, the peak observed at $1\,070\text{--}1\,020\text{ cm}^{-1}$ is assigned to the B—C bond. These are in accordance with the chemical structure of PBSZ.

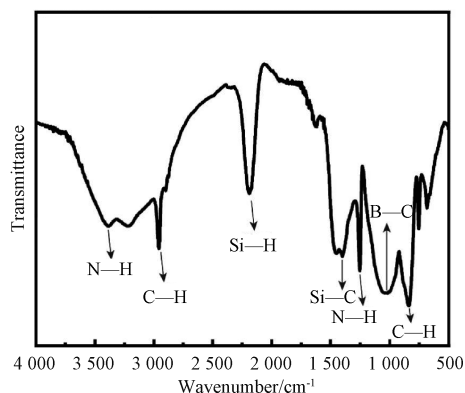


Fig. 1 FTIR spectrum of PBSZ synthesized at $250\text{ }^\circ\text{C}$

Figure 2 represents the FTIR spectra of PBSZ synthesized at different temperatures. The stretching vibration peak of Si—H becomes weak at $230\text{ }^\circ\text{C}$ and $250\text{ }^\circ\text{C}$ as compared to that of $200\text{ }^\circ\text{C}$, which indicates the synthesis of PBSZ via dehydrogenation coupling between Si—H and N—H. The mass fractions of the elements in PBSZ at different synthesis temperatures are shown in Table 1.

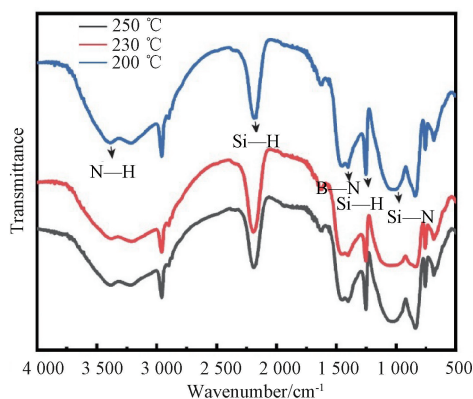


Fig. 2 FTIR spectra of PBSZ synthesized at 200, 230 and $250\text{ }^\circ\text{C}$

Table 1 Mass fractions of elements in PBSZ at different synthesis temperatures

Synthesis temperature/ $^\circ\text{C}$	Mass fraction/%				
	Si	B	N	C	H
200	42.33	4.19	17.73	27.13	8.62
230	41.84	4.21	18.56	26.89	8.50
250	41.55	4.25	18.99	26.78	8.43

2.2 NMR analysis of PBSZ

The NMR spectra of PBSZ are shown in Fig. 3, where δ denotes the chemical shift multiplied by 10^6 . Figure 3 (a) represents the spectrum of $^1\text{H-NMR}$. The peaks at $\delta = 4.5$ – 5.0 and 0.6 are attributed to the bonds of Si-H and N-H , respectively. The strong peak at $\delta = 0 - 0.45$ belongs to Si-CH_3 group. Figure 3 (b) represents the spectrum of $^{13}\text{C-NMR}$. The broad peaks at $\delta = 0$ – 5.0 are related to the Si-CH_3 group, and Si-CH_3 is the only form in which the C element could be

released while synthesizing at high temperatures. In $^{11}\text{B-NMR}$ spectrum, the signal of the BN_3 sites appears at $\delta = 27.2$, as shown in Fig. 3(c). The signals at $\delta = 3.4$ and $\delta = 3.5$ in the $^{29}\text{Si-NMR}$ spectrum (Fig. 3(d)) are attributed to the SiC_3N sites and the $\text{SiC}_2^{(\text{sp}^3)}\text{N}_2$ sites^[18], respectively, while the signal at $\delta = -38.0$ is assigned to the $\text{SiC}_2^{(\text{sp}^3)}\text{N}_3$ sites. The $^{29}\text{Si-NMR}$ spectrum reveals that the transformation of the sp^2 hybridized carbons of the vinyl groups into sp^3 carbons is due to the hydroboration and vinyl polymerization reactions occurring under certain conditions.

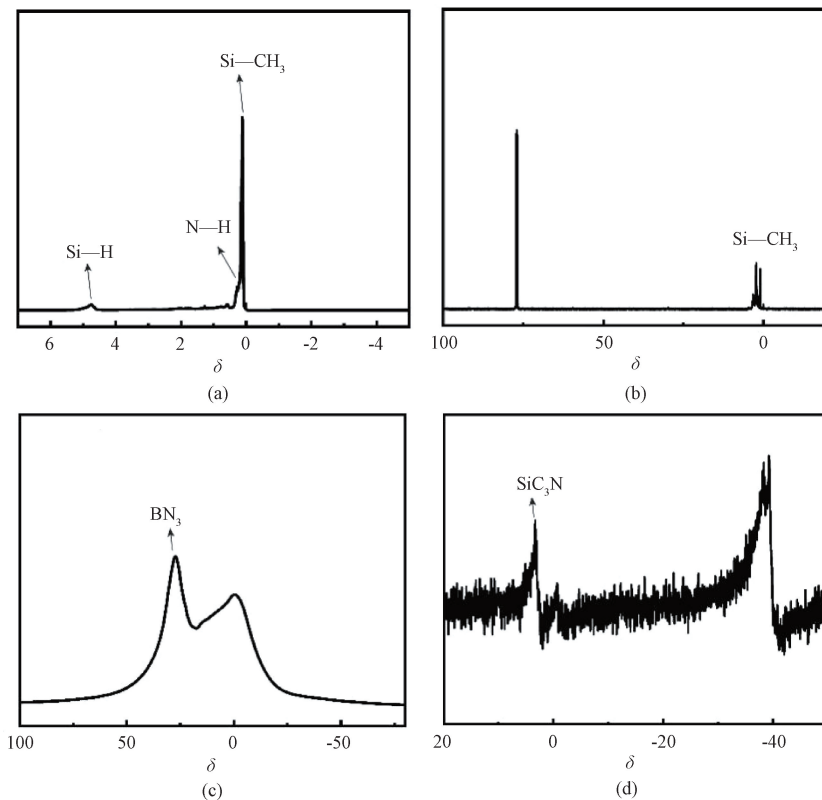


Fig. 3 NMR spectra of PBSZ: (a) $^1\text{H-NMR}$; (b) $^{13}\text{C-NMR}$; (c) $^{11}\text{B-NMR}$; (d) $^{29}\text{Si-NMR}$

2.3 XPS analysis of PBSZ

XPS analysis is shown in Fig. 4. Si, N and B elements are fitted according to the Gaussian function to explore the existing form and the binding state of each element in PBSZ. Figure 4(a) shows that the Si element exists primarily in three forms in PBSZ: Si-C (101.1 eV), Si-N (101.9 eV) and Si-O (100.0 eV). Partial oxidation of PBSZ during the experiment results in the formation of Si-O . The N1s spectra, like the Si2p spectra, have three peaks, N-H (399.0 eV), N-Si (398.3 eV) and N-B (398.3 eV), as shown in

Fig. 4(b). In the B1s spectrum, the only peak at 191.1 eV belongs to the B-N bond, which represents its presence in PBSZ. This indicates that these atoms are incorporated into the ceramics successfully as shown in Fig. 4 (c). XPS shows that multi-phase PBSZ is formed as shown in Fig. 4 (d). It can be seen from Fig. 4 (d) that O1s occurs at 545.4 eV, N1s at 395.4 eV, C1s at 280.0 eV, B1s at 190.8 eV, Si2s at 180.4 eV and Si2p at 99.0 eV. The results indicate that the network of Si-N-B and six-membered B-N rings are presented in PBSZ structure.

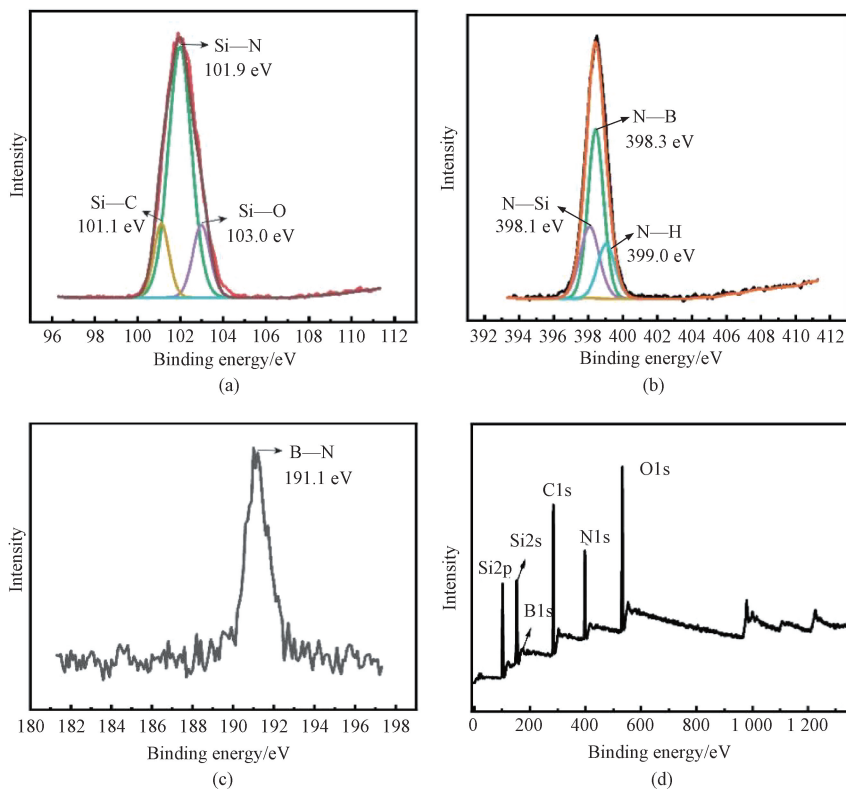


Fig. 4 XPS analyses: (a) Si; (b) N1s; (c) B1s; (d) PBSZ

2.4 Thermal analysis of PBSZ

Figure 5 shows the TGA of PBSZ, for the analysis of the mass loss of PBSZ^[19]. The ceramics yield of PBSZ at 800 °C in a Nitrogen atmosphere was 53.9%. The thermal mass loss of PBSZ is mainly divided into two stages. The first stage is from room temperature (RT) up to 200 °C, and the mass loss is about 6%. The main reason for the mass loss in this process is the removal of unreacted small molecules, such as $\text{Me}_6\text{Si}_2\text{NH}$ and Me_3SiCl . The second stage is from 200 °C to 550 °C, and the mass loss is about 36%. The mass loss in the first part of this stage is relatively fast, mainly due to the transamination reaction and cross-linking reaction of PBSZ, reaching a highly cross-linked state. The second part of the mass loss is mainly due to the organic-to-inorganic conversion reaction. A small number of methyl radicals and hydrogen radicals combine to generate methane and hydrogen. When the temperature is above 700 °C, there is nearly no mass loss, indicating that the polymer-to-ceramic transformation has been essentially completed.

The density of PBSZ synthesized at 250 °C is shown in Table 2. As can be seen from Table 2, the average density of PBSZ at RT is 1.03 g/cm³. Figure 6 shows the DSC heating curve of PBSZ prepared at a synthesis temperature of 250 °C and with a synthesis time of 3 h. It can be seen from Fig. 6 that the glass transition temperature of PBSZ synthesized at 250 °C is about 79 °C. In addition, with the increase in temperature,

there is no obvious melting peak but a line extending in the endothermic direction, which indicates that PBSZ is amorphous.

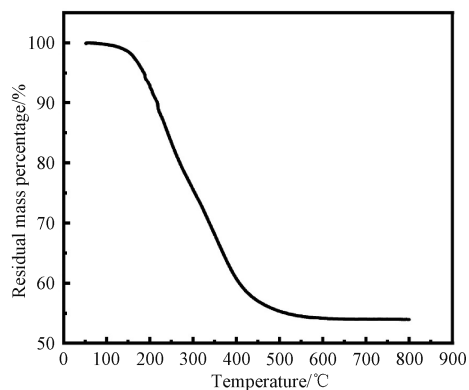


Fig. 5 TGA of PBSZ from RT to 800 °C

Table 2 PBSZ density

Number	Volume/cm ³	Density/(g/cm ³)
1	1.93	1.03
2	1.92	1.03
3	1.92	1.04
Average	1.92	1.03

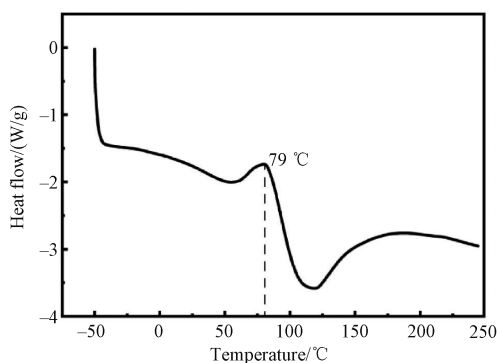


Fig. 6 DSC curve of PBSZ synthesized at 250 °C

3 Conclusions

The SiBNC ceramic precursor, PBSZ, was successfully synthesized by using BCl_3 , HSiCl_3 and $\text{Me}_6\text{Si}_2\text{NH}$ as raw materials through the PDCs method. FTIR and NMR spectra show that Si—N, N—H and B—N bonds are in the structure. TGA indicates that PBSZ contains a ceramic yield of about 53.9% at 800 °C in a nitrogen atmosphere. In addition, the results show that PBSZ is amorphous and the network of Si—N—B and six-membered B—N rings are presented in PBSZ structure. Thus, the study indicates that PBSZ is suitable for producing high-performance SiBNC ceramics.

References

[1] KAMAL A, RAJASEKHAR B V, PAINULY A, et al. A novel precursor for the synthesis of mixed non-oxide ultra high temperature ceramics [J]. *Journal of Inorganic and Organometallic Polymers and Materials*, 2020, 30 (5): 1578-1588.

[2] JI X Y, SHAO C W, WANG H, et al. A simple and efficient method for the synthesis of SiBNC ceramics with different Si/B atomic ratios [J]. *Ceramics International*, 2017, 43 (10): 7469-7476.

[3] LEE J, BUTT D P, BANEY R H, et al. Synthesis and pyrolysis of novel polysilazane to SiBCN ceramic [J]. *Journal of Non-Crystalline Solids*, 2005, 351 (37/38/39): 2995-3005.

[4] YU Z J, PEI Y X, LAI S Y, et al. Single-source-precursor synthesis, microstructure and high temperature behavior of TiC-TiB₂-SiC ceramic nanocomposites [J]. *Ceramics International*, 2017, 43(8): 5949-5956.

[5] ZHANG L S, TANG Z C, TUSIIME R, et al. Synthesis and electromagnetic wave absorbing properties of a polymer-derived SiBNC ceramic aerogel [J]. *Ceramics International*, 2021, 47 (13): 18984-18990.

[6] LUAN X G, GU S M, ZHANG Q Q, et al. An electrically conductive SiBCN film prepared via polymer-derived ceramic and chemical vapor deposition methods [J]. *Sensors and Actuators A: Physical*, 2021, 330: 112824.

[7] YUAN W, WANG Y, LUO Z, et al. Improved performances of SiBCN powders modified phenolic resins-carbon fiber composites [J]. *Processes*, 2021, 9(6): 955.

[8] ZHAO H, CHEN L X, LUAN X G, et al. Synthesis, pyrolysis of a novel liquid SiBCN ceramic precursor and its application in ceramic matrix composites [J]. *Journal of the European Ceramic Society*, 2017, 37(4): 1321-1329.

[9] PUERTA A R, REMSEN E E, BRADLEY M G, et al. Synthesis and ceramic conversion reactions of 9-BBN-modified allylhydridopolycarbosilane; a new single-source precursor to boron-modified silicon carbide [J]. *Chemistry of Materials*, 2003, 15(2): 478-485.

[10] GE Y Y, SUN S Y, WANG Q, et al. Effect of Fe-contained species on the preparation of α -Si₃N₄ fibers in combustion synthesis [J]. *Journal of the American Ceramic Society*, 2016, 99(4): 1464-1471.

[11] SHEN Z E, REN S, GE C, et al. Recent progress on fabrication of thermal conductive aluminum nitride fibers [J]. *Journal of Donghua University(English Edition)*, 2023, 40(6): 622-630.

[12] COLOMBO P, MERA G, RIEDEL R, et al. Polymer-derived ceramics; 40 years of research and innovation in advanced ceramics [J]. *Journal of the American Ceramic Society*, 2010, 93(7): 1805-1837.

[13] WANG Y, CHEN L X, XU T T, et al. High char yield novolac modified by Si-B-N-C precursor: thermal stability and structural evolution [J]. *Polymer Degradation and Stability*, 2017, 137: 184-196.

[14] ZHANG Q, YANG Z H, JIA D C, et al. Synthesis and structural evolution of dual-boron-source-modified polysilazane derived SiBCN ceramics [J]. *New Journal of Chemistry*, 2016, 40(8): 7034-7042.

[15] KONG J, WANG M J, ZOU J H, et al. Soluble and meltable hyperbranched polyborosilazanes toward high-temperature stable SiBCN ceramics [J]. *ACS Applied Materials & Interfaces*, 2015, 7(12): 6733-6744.

[16] BERNARD S, WEINMANN M, CORNU D, et al. Preparation of high-temperature stable SiBCN fibers from tailored single source polyborosilazanes [J]. *Journal of the European Ceramic Society*, 2005, 25(2/3): 251-256.

[17] JÄSCHKE T, JANSEN M. Synthesis and characterization of new amorphous Si/B/N/C

- ceramics with increased carbon content through single-source precursors [J]. *Comptes Rendus-Chimie*, 2004, 7(5): 471-482.
- [18] YUAN J, HAPIS S, BREITZKE H, et al. Single-source-precursor synthesis of hafnium-containing ultrahigh-temperature ceramic nanocomposites (UHTC-NCs) [J]. *Inorganic Chemistry*, 2014, 53(19): 10443-10455.
- [19] GU J W, LIANG C B, DANG J, et al. Ideal dielectric thermally conductive bismaleimide nanocomposites filled with polyhedral oligomeric silsesquioxane functionalized nanosized boron nitride [J]. *RSC Advances*, 2016, 6(42): 35809-35814.

硅硼碳氮陶瓷前驱体聚硼硅氮烷的合成与表征

MALIK Hamza¹, 申 键¹, 唐滋成¹, 刘 勇^{1,2*}

1. 东华大学 材料科学与工程学院 纤维材料改性国家重点实验室, 上海 201620
2. 东华大学 高性能纤维及制品教育部重点实验室, 上海 201620

摘要: 以三氯化硼 (BCl_3)、三氯硅烷 (HSiCl_3) 和六甲基二硅氮烷 ($\text{Me}_6\text{Si}_2\text{NH}$) 为原料, 通过聚合物前驱体转化陶瓷 (polymer-derived ceramics, PDCs) 法成功合成了硅硼碳氮 (SiBNC) 陶瓷前驱体——聚硼硅氮烷 (PBSZ)。采用傅里叶变换红外光谱、核磁共振、X 射线光电子能谱、热重分析和差示扫描量热对 PBSZ 的结构和热性能进行分析。结果表明, PBSZ 结构中存在硅氮硼 (Si—N—B) 网络和六元硼氮 (B—N) 环。在氮气中, 800 °C 时 PBSZ 的陶瓷产率为 53.9%。

关键词: 硅硼碳氮 (SiBNC) 陶瓷; 陶瓷前驱体; 聚硼硅氮烷 (PBSZ); 聚合物前驱体转化陶瓷 (PDCs) 法